
Surgical Post-Training: Cutting Errors, Keeping Knowledge

Wenye Lin¹Kai Han^{1*}

Abstract

Enhancing the reasoning capabilities of Large Language Models (LLMs) via post-training is often constrained by the trade-off between efficiency and catastrophic forgetting. While prior research emphasizes the role of on-policy data in mitigating forgetting, we uncover—and validate both theoretically and empirically—an overlooked yet critical mechanism: the implicit regularization inherent in Direct Preference Optimization’s (DPO) reward estimate. This motivates our Surgical Post-Training (SPoT), a new paradigm designed to optimize reasoning efficiently while preserving learned prior knowledge. SPoT consists of: (1) a data rectification pipeline that employs an Oracle to surgically correct erroneous steps via minimal edits, generating data proximal to the model’s distribution; and (2) a reward-based binary cross-entropy objective. Unlike the relative ranking in DPO, this objective treats reasoning correctness as a binary classification problem, enforcing decoupled supervision signals. Empirically, with only 4k rectified math data pairs, SPoT improves Qwen3-8B’s accuracy by 6.2% on average across in-domain and OOD tasks, requiring merely 28 minutes of training on 8× H800 GPUs. Code: <https://github.com/Visual-AI/SPoT>

1. Introduction

While pretraining establishes the foundation of Large Language Models (LLMs) (Achiam et al., 2023; Comanici et al., 2025; Yang et al., 2025), the post-training phase remains critical for eliciting specific competencies, such as mathematical reasoning (Shao et al., 2024), code generation (Anthropic, 2024), and human alignment (Ouyang et al., 2022; Zhou et al., 2023). Post-training for reasoning typically follows two primary paradigms: Supervised Fine-Tuning (SFT) and Reinforcement Learning (RL). While SFT ben-

efits from strong supervision, it is often compromised by catastrophic forgetting of the model’s prior knowledge (Chu et al., 2025; Huan et al., 2025). Conversely, on-policy RL methods like Group Relative Policy Optimization (GRPO) (Shao et al., 2024) effectively mitigate forgetting but incur substantial computational overhead during the rollout process. More critically, standard RL is constrained by its reliance on the base model’s ability to sample correct reasoning paths, preventing it from expanding the model’s fundamental reasoning boundaries (Yue et al., 2025).

This trade-off raises a critical question: *Can we unite the efficiency of SFT with the generalization capabilities of RL without sacrificing performance?* Addressing this challenge necessitates a deeper understanding of the mechanisms behind catastrophic forgetting. A prevailing view attributes the poor generalization of SFT to drastic distributional shift between the training data and the model’s policy (Chen et al., 2025; Shenfeld et al., 2025). To bridge the gap, we introduce a data rectification pipeline designed to generate proximal-distribution data. We employ an Oracle (e.g., a stronger teacher model) to surgically correct erroneous outputs via minimal edits, yielding positive samples that remain proximal to the model’s original distribution.

However, we find that data proximity is necessary but insufficient. Empirically, SFT on this proximal data *still* incurs forgetting, whereas Direct Preference Optimization (DPO) (Rafailov et al., 2023) does not. To understand the mechanism, we employ a Reward-SFT baseline, a method integrating the DPO reward formulation into SFT. We observe that Reward-SFT effectively retains prior knowledge, confirming that *the KL-constraint in the reward definition* is the decisive factor, by “tethering” the updated policy to the reference model. While preserving prior knowledge is essential, the model must also drive superior gains in in-domain reasoning. We identify two failure modes: (1) *the “pull-up” effect* (Ren & Sutherland, 2025) inherent in positive-only training (e.g., SFT), which inadvertently raises the likelihood of erroneous responses alongside correct ones; and (2) *the inadequacy of relative ranking* in DPO for reasoning with rigid correctness.

To address these limitations, we propose Surgical Post-Training (SPoT), a paradigm designed to optimize reasoning efficiently while preserving prior knowledge. SPoT

*Corresponding author. ¹The University of Hong Kong. Correspondence to: Kai Han <kaihanx@hku.hk>, Wenye Lin <linius@connect.hku.hk>.

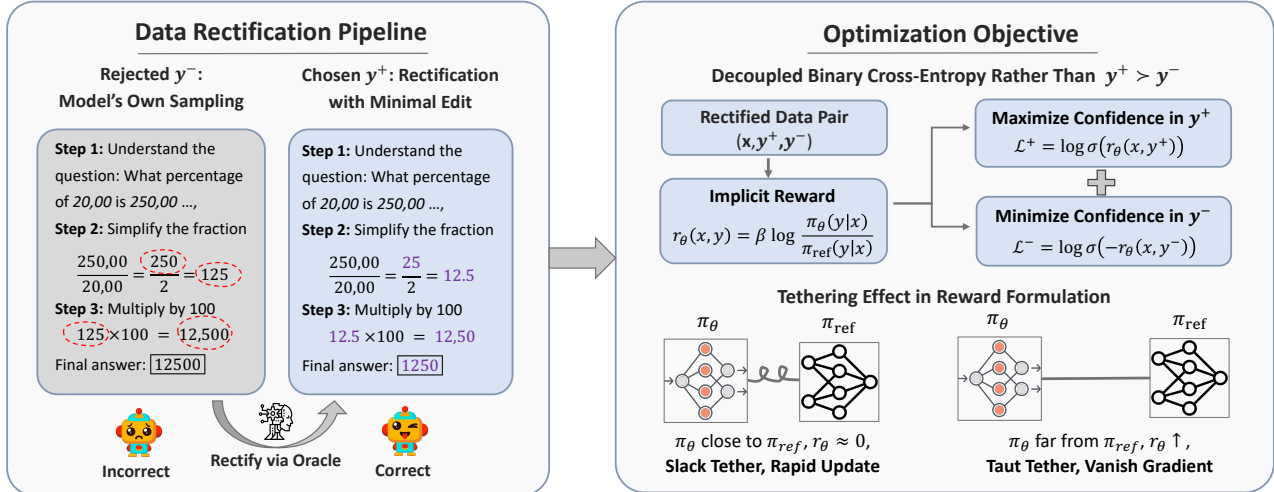


Figure 1. **Illustration of SPOT.** Left: Our framework utilizes an Oracle to apply surgical rectifications to erroneous reasoning steps, generating positive samples that remain proximal to the model’s original distribution. Top-Right: Unlike the relative ranking used in DPO, we leverage an explicit classification objective that proves more effective for reasoning tasks. Bottom-Right: The tethering effect inherent in our reward definition effectively mitigates catastrophic forgetting.

integrates our data rectification pipeline with a reward-based binary cross-entropy objective to maintain the “tethering” effect of the reference model. Distinct from the relative ranking in DPO, our objective explicitly maximizes the likelihood of the rectifications while suppressing errors.

Our contributions are summarized as follows:

1. We demonstrate that beyond on-policy data, implicit regularization is another critical factor in mitigating forgetting. We show that with identical data, SFT fails to generalize, whereas DPO retains previous knowledge.
2. We identify the “pull-up” effect in positive-only training, and insufficiency of DPO for rigid reasoning tasks. We then validate a binary classification objective that provides a denser signal.
3. We propose SPOT, a computationally efficient paradigm that mitigates catastrophic forgetting by synergizing minimal-edit data rectification with a reward-based objective. We validate our method on Qwen3-8B and Llama-3.1-8B-Instruct, demonstrating consistent improvements and robust generalization.
4. To strictly evaluate out-of-domain (OOD) reasoning without data contamination, we also leverage GAME-BoT (Lin et al., 2025) to dynamically construct a Connect4 dataset for reliable evaluation.

2. Data Rectification Pipeline

Our SPOT framework consists of two core components: a *data rectification pipeline* and a *specialized optimization*

objective (see Fig. 1). In this section, we detail the first component designed to produce valid reasoning paths proximal to the model’s distribution.

Standard SFT often utilizes offline datasets that diverge significantly from the model’s current policy π_θ , leading to catastrophic forgetting (Chen et al., 2025). Conversely, on-policy methods rely entirely on the model’s intrinsic probability of sampling correct reasoning paths, making them inefficient for hard reasoning tasks. For example, if a model’s pass rate on a specific problem is 1%, obtaining a single correct response requires an expected 100 rollouts, which is computationally expensive. Furthermore, for problems beyond the model’s current capabilities, self-sampling fails to yield any training signal, making it impossible to learn from those instances (Yu et al., 2025).

To bridge this gap, we propose a *data rectification pipeline* to construct a contrastive dataset $\mathcal{D} = \{(x, y^-, y^+)\}$ where the positive response y^+ only perform necessary correction of erroneous logic of the negative response y^- while preserving the model’s original generation style and lexical structure. An example is shown in Fig. 1. The pipeline consists of the following three stages:

Error Elicitation We first construct a dataset of model failures. Given a question x from the dataset, we sample a response y^- from the current policy: $y^- \sim \pi_\theta(\cdot|x)$. We evaluate y^- against the ground-truth answer. If the final answer is incorrect, we retain the pair (x, y^-) for rectification.

Oracle-Guided Surgical Rectification We employ an Oracle to perform surgical edits, which can be either a human being or a stronger teacher model. The Oracle is provided

with y^- and optionally the ground truth, then instructed to only modify incorrect reasoning steps, while maintaining the original style. This results in a rectified response y^+ that represents the “nearest valid neighbor” to the error y^- in the semantic space. To enhance efficiency, we adopt an *offline* setting. We provide the full prompts in Appendix F.

LCS Filtering To strictly enforce the proximity of the rectified data to the student’s distribution, we apply a topological constraint based on the Longest Common Subsequence (LCS) (Wagner & Fischer, 1974). For every pair (y^-, y^+) , we calculate the change ratio R_{LCS} :

$$R_{LCS}(y^-, y^+) = 1 - \frac{|\text{LCS}(y^-, y^+)|}{|y^+|}, \quad (1)$$

where $|\cdot|$ denotes sequence length. We filter out samples where $R_{LCS} > \gamma$. We set $\gamma = 0.6$ to maximize the retention of training samples while maintaining model performance. Appendix D shows the change ratio distributions.

In the resulting dataset, y^- and y^+ in each sample share the majority of their token trajectories, diverging only at decision-critical parts. This is essential for our subsequent optimization, as it allows the gradients to focus more on the divergent reasoning tokens.

3. The Reward Is Secretly a Regularizer

Building upon the proximal dataset constructed via the pipeline in Section 2, in this section, we demonstrate that data proximity alone is insufficient to prevent catastrophic forgetting. We analyze the learning dynamics of SFT versus reward-based methods, showing that the learning objective itself serves as an intrinsic regularizer against forgetting.

3.1. Empirical Observation: The Regularization Gap

We conduct controlled experiments using the English subset of DAPO-Math-17k (Yu et al., 2025). Leveraging our pipeline, we generate 4k contrastive pairs by employing Qwen3-8B as the base policy π_θ and Gemini 2.5 Pro as the Oracle for rectification. We compare the following methods trained on $\mathcal{D} = \{(x, y^-, y^+)\}$ and evaluate OOD generalization using IFEval (Zhou et al., 2023):

SFT+ To distinguish from standard fine-tuning on raw off-policy data, we refer to Supervised Fine-Tuning performed on the surgically rectified positive samples y^+ as SFT+, which minimizes the same negative log-likelihood as SFT:

$$\mathcal{L}_{\text{SFT}} = -\mathbb{E}_{x, y^+ \sim \mathcal{D}}[\log \pi_\theta(y^+ | x)] \quad (2)$$

DPO DPO optimizes a policy by leveraging a relative ranking objective derived from an implicit reward $r_\theta(x, y)$.

It is defined as the log-ratio between the policy π_θ and the frozen reference model π_{ref} (initialized with the same parameters as π_θ), scaled by a coefficient β :

$$r_\theta(x, y) = \beta \log \frac{\pi_\theta(y|x)}{\pi_{\text{ref}}(y|x)} \quad (3)$$

DPO maximizes the margin between the chosen response y^+ and the rejected response y^- :

$$\mathcal{L}_{\text{DPO}} = -\mathbb{E}_{x, y^+, y^- \sim \mathcal{D}}[\log \sigma(r_\theta(x, y^+) - r_\theta(x, y^-))] \quad (4)$$

Reward-SFT We introduce Reward-SFT as a control baseline to isolate the effect of the implicit reward from the influence of negative samples. Unlike SFT, which optimizes the likelihood of tokens directly, this objective simply maximizes the probability of the chosen response y^+ being classified as “correct” under the implicit reward formulation:

$$\mathcal{L}_{\text{RW-SFT}} = -\mathbb{E}_{x, y^+ \sim \mathcal{D}}[\log \sigma(r_\theta(x, y^+))] \quad (5)$$

Functionally, this treats the optimization as a binary classification task where the model learns to classify y^+ as “high reward” relative to the reference distribution.

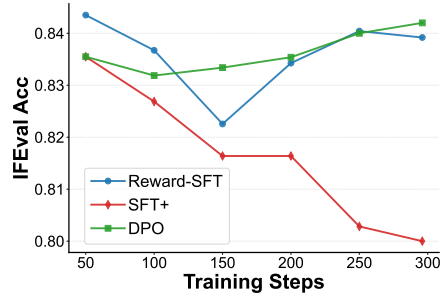


Figure 2. **IFEval Acc Results (avg@5)**. SFT+ forgets instruction following ability, while reward-based methods do not.

As illustrated in Figure 2, a significant divergence in generalization capability is observed. SFT+ suffers from immediate catastrophic forgetting, with IFEval performance decaying monotonically as training progresses. DPO remains stable and even gains slight improvements. Crucially, similar to SFT+, Reward-SFT does not see negative data, yet it matches the OOD stability of DPO. This finding suggests that *the resistance to forgetting stems from the implicit regularization inherent in the reward formulation*.

3.2. Gradient Analysis: The Mechanics of Tethering

To understand why Reward-SFT prevents forgetting while standard SFT objective fails, we analyze the gradient dynamics of their respective loss functions. **We show that the distinction between these two objectives lies entirely in the dynamic scaling coefficient of the gradient.**

The gradient for SFT with respect to the model parameters θ is:

$$\nabla_{\theta} \mathcal{L}_{\text{SFT}} = -\nabla_{\theta} \log \pi_{\theta}(y^+|x) \quad (6)$$

Meanwhile, the gradient for Reward-SFT in Equation (5) includes a dynamic re-weighting coefficient determined by r_{θ} from Equation (3):

$$\begin{aligned} \nabla_{\theta} \mathcal{L}_{\text{RW-SFT}} &= -\frac{\partial \log \sigma(r)}{\partial r} \nabla_{\theta} r_{\theta}(x, y^+) \\ &= -(1 - \sigma(r_{\theta}(x, y^+))) \cdot \beta \nabla_{\theta} \log \pi_{\theta}(y^+|x) \quad (7) \end{aligned}$$

Comparing Equation (6) and Equation (7) reveals a fundamental difference in optimization pressure. In standard SFT, the gradient is scaled by a constant coefficient of 1. Consequently, SFT applies uniform optimization pressure to all samples, regardless of the model’s current competence. Even if the model has effectively assigned high probability to the training sample (e.g., $p(y^+|x) \approx 0.99$), the SFT objective continues to force parameter updates to push the probability toward 1.0. This unbounded optimization compels the model to overwrite its pre-trained features, resulting in significant distribution shift and loss of prior capabilities.

In contrast, Reward-SFT introduces an instance-dependent dynamic scaling coefficient $\lambda(x, y^+) = 1 - \sigma(r_{\theta}(x, y^+))$ (For simplicity, we assume $\beta = 1$ in our analysis). We term λ the *Elastic Tether*, as it modulates the “tension” of gradient updates. Functioning as an adaptive regularizer based on the implicit reward value, it creates two distinct modes of training:

- **Acquisition Mode (Slack Tether):** Initially, when the policy π_{θ} is close to the reference π_{ref} , the reward $r_{\theta} \approx 0$ and the scaling factor $\lambda \approx 0.5$. In this regime, the Elastic Tether is slack, allowing the model to rapidly adapt to the preferred response distribution.
- **Saturation Mode (Taut Tether):** As the model aligns with the target and the implicit reward r_{θ} increases, the scaling coefficient vanishes due to the saturation property of the sigmoid function:

$$\lim_{r_{\theta} \rightarrow \infty} \lambda(x, y^+) = \lim_{r_{\theta} \rightarrow \infty} (1 - \sigma(r_{\theta})) = 0$$

Analogous to the increasing tension of a physical tether, this mechanism restricts the policy model from deviating excessively from the reference model.

Consider a sample where the model has achieved high confidence relative to the reference, yielding a reward of $r_{\theta} = 10$. The sigmoid function saturates, and the gradient scaling coefficient λ becomes:

$$\lambda = 1 - \sigma(10) = 1 - \frac{1}{1 + e^{-10}} \approx 4.5 \times 10^{-5}$$

In comparison to standard SFT, where the coefficient is fixed at 1.0, the Elastic Tether tightens the constraint by a factor of over 20,000. This drastic reduction suppresses the gradient signal, preventing the “over-optimization” that causes the model to drift from its pre-trained knowledge.

The Elastic Tether enables a self-regulating process that halts optimization once the policy is sufficiently distinguished from the reference distribution. **This acts as an automatic, sample-wise early stopping mechanism.** By tethering the updated policy to the reference model and suppressing updates on well-learned samples, Reward-SFT thereby preserves the pre-trained knowledge inherent in π_{ref} .

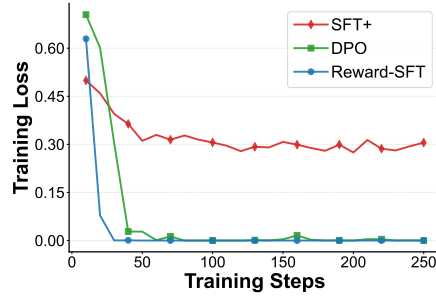


Figure 3. **Training loss curve.** Reward-SFT and DPO converge rapidly to near-zero as the policy satisfies the relative margin constraint. SFT+ remains high as it attempts to maximize absolute likelihood, driving continuous parameter updates.

These theoretical insights are empirically substantiated by the training loss trajectories in Fig. 3 and the reward evolution in Fig. 4. As shown in Fig. 3, the Reward-SFT loss rapidly converges to zero. This behavior is a direct consequence of the definition in Eq. (5): as $r_{\theta}(x, y^+)$ increases, $\mathcal{L}_{\text{RW-SFT}}$ approaches zero. In contrast, the SFT objective drives continuous optimization, forcing superfluous parameter updates that degrade general capabilities. Furthermore, the reward trajectories in Fig. 4 align perfectly with our gradient analysis. As r_{θ} grows, the gradient of Reward-SFT vanishes. Consequently, the reward for chosen responses under Reward-SFT plateaus, whereas the SFT counterpart continues to rise unbounded. **In contrast to recent work suggesting that KL-divergence fails to mitigate forgetting (Chen et al., 2025; Shenfeld et al., 2025), these analyses corroborate the critical role of KL-constrained reward formulation in keeping knowledge during post-training.**

4. The Surgical Optimization Objective

While preserving prior knowledge is essential, it is insufficient; the model must also achieve substantial in-domain reasoning improvements. This section uncovers the specific failure modes hindering this goal: the “pull-up” effect inherent in positive-only training (e.g., SFT, Reward-SFT) and the inadequacy of relative ranking (DPO) for reasoning

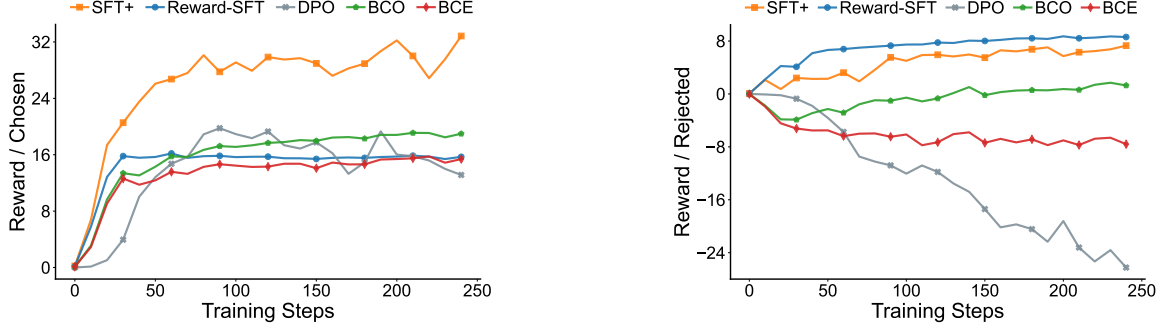


Figure 4. **Evolution of implicit rewards during training.** Left: reward scores for chosen responses; Right: reward scores for rejected responses. The reward shows how much the model’s preference for the selected response has increased compared to its initial stage.

with verifiable truth. To bridge this gap, we introduce a reward-based binary cross-entropy objective.

4.1. The “Pull-Up” Effect

While Reward-SFT effectively utilizes the “Elastic Tether” to prevent forgetting, it inherits a similar susceptibility from standard SFT when training on our surgical rectification data. As shown in the right panel of Fig. 4, although we conduct training only on chosen data y^+ , **the likelihood of rejected responses y^- for both SFT+ and Reward-SFT inadvertently rises relative to the reference model.**

This effect is termed “pull-up” by Ren & Sutherland (2025): under *only positive* supervision, the model indiscriminately increases the probability mass of the target distribution, reinforcing similar but unwanted responses. Since our rectification pipeline generates y^+ and y^- sharing the vast majority of their token trajectory, maximizing the likelihood of y^+ inevitably boosts the probability of y^- . Consequently, the model fails to establish a sharp decision boundary at the critical point of divergence, underscoring the necessity of negative samples to suppress unwanted generation paths.

4.2. The Insufficiency of Relative Ranking

Given the need for negative supervision, DPO appears to be a natural candidate. DPO models preference probabilities using the Bradley-Terry model (Bradley & Terry, 1952), minimizing the negative log-likelihood of the margin $M = r_\theta(x, y^+) - r_\theta(x, y^-)$:

$$P(y^+ \succ y^-) = \sigma(r_\theta(x, y^+) - r_\theta(x, y^-)) \quad (8)$$

However, this relative ranking formulation is unsuitable for reasoning where the answer is strictly right or wrong. In preference alignment tasks (e.g., creative writing), it suffices for a response to be *better* than the alternative. Differently, in reasoning, a step is objectively *correct* or *incorrect*. The model is expected to maximize the probability of the correct response y^+ while suppressing the incorrect one y^- .

While gradient descent naturally follows the path of least resistance, the DPO loss can be minimized by decreasing the rejected reward $r(x, y^-)$ while leaving the chosen reward $r(x, y^+)$ stagnant—or even allowing it to drop, provided $r(x, y^-)$ drops faster. This phenomenon is observed in Rafailov et al. (2024); Pal et al. (2024); Ren & Sutherland (2025), and also corroborated by our results in Fig. 4: at later stage of DPO’s training, the reward for chosen responses fails to show sustained growth, while the reward for rejected ones decreases drastically. This suggests DPO tends to optimize the margin by suppressing y^- rather than reinforcing correct logic, rendering it insufficient for reasoning tasks.

4.3. Reward-based Binary Cross Entropy Optimization

To address these limitations, we reframe reasoning optimization as a binary classification task. Unlike DPO, which relies on the relative ranking between pairs, we decouple the supervision into independent positive and negative terms. We introduce two variants:

SPoT-BCE By decoupling the DPO objective in Eq. (4), we enforce the model to independently maximize confidence in y^+ and minimize confidence for y^- . This results in the standard Binary Cross Entropy (BCE) loss:

$$\mathcal{L}_{\text{SPoT-BCE}} = -\mathbb{E}_{\mathcal{D}}[\log \sigma(r_\theta(x, y^+)) + \log \sigma(-r_\theta(x, y^-))] \quad (9)$$

The implicit reward $r_\theta(x, y)$ here serves as the classification logit. This formulation provides a dense supervision signal while effectively retaining pre-trained knowledge.

SPoT-BCO While Binary Classifier Optimization (BCO) (Jung et al., 2025) was originally designed for unpaired data (e.g., thumbs-up/down only), we identify it as uniquely suitable for our paired reasoning data. BCO introduces a reward-shift δ to the BCE loss:

$$\mathcal{L}_{\text{SPoT-BCO}} = -\mathbb{E}_{x, y^+, y^- \sim \mathcal{D}}[\log \sigma(r_\theta(x, y^+) - \delta) + \log \sigma(-(r_\theta(x, y^-) - \delta))] \quad (10)$$

where $\delta = \frac{1}{2} \cdot \mathbb{E}_{x, y^+, y^- \sim \mathcal{D}}[r_\theta(x, y^+) + r_\theta(x, y^-)]$. In practice, δ is computed by an exponential moving average of the batch statistics.

4.4. Theoretical Analysis of δ

The difference between SPoT-BCE and SPoT-BCO lies in the reward shift δ . While Jung et al. (2025) frame δ as providing a tighter upper bound of DPO, we analyze its specific role in reasoning alignment from a different viewpoint.

The implicit reward $r_\theta(x, y)$ defined in Eq. (3) is a simplified version of the theoretical optimal reward $r'(x, y)$. The exact relationship derived from the KL-constrained optimal policy π^* is given by:

$$r'(x, y) = \beta \log \frac{\pi^*(y|x)}{\pi_{\text{ref}}(y|x)} + \beta \log Z(x) \quad (11)$$

where $Z(x)$ is the partition function. While DPO eliminates $\beta \log Z(x)$ via subtraction, BCO does not yield a similar subtraction. Comparing the implicit reward in Eq. (10) and Eq. (11) reveals that the shift term δ serves as a functional proxy for the intractable partition term $\beta \log Z(x)$.

Mitigating Saturation for In-Domain Reasoning As training progresses, the average implicit rewards r_θ may increase (see Fig. 4). In SPoT-BCE ($\delta = 0$), these elevated scores push the sigmoid input into saturation ($\sigma(\cdot) \rightarrow 1$), causing gradients to vanish. This saturation may halt optimization prematurely. By adapting δ via the exponential moving average, SPoT-BCO dynamically adjusts the threshold to enable further update for the positive term $\log \sigma(r_\theta(x, y^+) - \delta)$, resulting in higher rewards for chosen responses compared to SPoT-BCE (see Fig. 4) and consequently better performance on in-domain reasoning tasks.

The Trade-off with OOD Generalization Meanwhile, the early saturation in SPoT-BCE naturally limits the deviation of π_θ from π_{ref} . By relaxing this constraint, the adaptive shift in SPoT-BCO permits further optimization, leading to a larger KL divergence from the reference model. Consequently, SPoT-BCE retains prior knowledge more faithfully than SPoT-BCO.

4.5. Surgical Post-Training

Surgical Post-Training takes its name from the synergistic design of our data pipeline and optimization objective. (1) Our data pipeline yields a dataset where y^- and y^+ of each sample share the majority of their token trajectories, diverging only at decision-critical parts. (2) For the tokens within the shared prefix of y^+ and y^- , the gradients for the positive and negative terms counteract each other, suppressing updates on these tokens. Consequently, parameter updates concentrate more on the *divergent* tokens, acting as

a form of “surgery” for the model—precisely correcting the reasoning failure while minimizing impact on the original distribution.

Beyond this, SPoT offers distinct advantages in:

- **Data efficiency and knowledge injection.** While RL is limited by self-sampling and discards data beyond the model’s current ability, SPoT uses an Oracle to inject new knowledge, expanding the model’s capability boundary with better data utilization.
- **Training efficiency.** Sampling-based RL is costly, requiring many rollouts per question. In contrast, SPoT requires only one rollout per question and typically converges within two epochs. Furthermore, SFT operates offline without frequently waiting for online sampling.
- **Fine-grained supervision.** Standard RL risks unlearning correct steps by penalizing full trajectories for partial errors. SPoT provides fine-grained supervision by penalizing only the specific flawed steps.
- **Pipeline simplification.** Instead of a complex multi-phase post-training pipeline (SFT \rightarrow GRPO \rightarrow DPO), SPoT offers the potential for a single-phase approach, which we term *behavior calibration*, that optimizes reasoning and preference alignment simultaneously.

5. Experiments

In this section, we present the experimental results of SPoT, followed by ablation studies that validate the effectiveness of our optimization objective (Section 5.3) and our data pipeline (Section 5.4).

5.1. Setup

Models and Datasets We adopt Qwen3-8B and Llama3.1-8B-Instruct as the policy models for training. We intentionally choose instruction-tuned models over base models, since these already post-trained models are more susceptible to catastrophic forgetting (Lu & Lab, 2025). If SPoT retains these models’ prior knowledge during subsequent training, it validates the robustness of our approach. For Qwen3-8B, we enforce a non-thinking mode by explicitly inserting an empty thinking block (“<think>\n\n</think>\n\n”). We leverage Gemini 2.5 Pro as the Oracle for rectification.

Experiments are conducted using the English subset of DAPO-Math-17k (Yu et al., 2025). Leveraging our pipeline, we generate 4k contrastive pairs for Qwen3-8B. For Llama3.1-8B-Instruct model, we randomly sample 1.5k pairs, matching the number of correct responses the model could inherently generate, to ensure a fair comparison with Rejection sampling Fine-Tuning (RFT). All methods are compared using the same amount of training data.

Table 1. Main results for in-domain reasoning, OOD reasoning, and general instruction following (OOD non-reasoning). We compare SPoT (with BCO loss) against standard baselines: SFT (rejection-sampled Gemini 2.5 Pro responses), RFT (rejection-sampled self-generated responses), and SFT+ (rectified y^+). Direct SFT leads to performance degradation on both in-domain and OOD tasks. RFT fails to yield clear in-domain improvements and causes OOD regression. While SFT+ improves in-domain reasoning with near-distribution data, it still suffers OOD losses. In contrast, SPoT demonstrates superiority in both in-domain and OOD performance. We report avg@16 for AIME24, AIME25, and AMC23, and avg@5 for the others.

Model	In-domain Reasoning							OOD Reasoning			General	Avg
	AIME24	AIME25	AMC23	Math500	Minerva	Olympia	Avg	GPQA-D	Connect4	Avg	IFEval	
Qwen3-8b	22.0	19.3	66.5	82.8	37.9	52.3	46.8	48.9	10.9	29.9	83.0	47.1
Qwen3-8b+SFT	15.3	13.3	56.0	78.2	38.6	44.3	41.0 _{↓5.8}	39.0	12.0	25.5 _{↓4.4}	79.6 _{↓3.4}	41.8 _{↓5.3}
Qwen3-8b+RFT	27.3	20.0	59.0	83.0	40.4	53.8	47.3 _{↑0.5}	49.1	3.1	26.1 _{↓3.8}	81.5 _{↓1.5}	46.4 _{↓0.7}
Qwen3-8b+SFT+	29.3	24.7	67.3	84.8	42.5	54.5	50.5 _{↑3.7}	47.3	14.1	30.7 _{↑0.8}	80.0 _{↓3.0}	49.4 _{↑2.3}
Qwen3-8b+SPoT	28.0	27.3	71.5	87.4	39.7	58.5	52.1 _{↑5.3}	46.8	36.0	41.4 _{↑11.5}	84.8 _{↑1.8}	53.3 _{↑6.2}
Llama3.1-8b-Instruct	3.3	2.7	19.5	47.0	22.4	16.9	18.6	28.5	5.0	16.8	73.6	24.3
Llama3.1-8b-Instruct+SFT	3.3	2.0	21.5	46.8	19.5	15.1	18.0 _{↓0.6}	29.6	1.7	15.7 _{↓1.1}	62.1 _{↓11.5}	22.4 _{↓1.9}
Llama3.1-8b-Instruct+RFT	3.3	0.0	24.0	46.0	19.1	15.3	18.0 _{↓0.6}	32.3	2.0	17.2 _{↑0.4}	71.2 _{↓2.4}	23.7 _{↓0.6}
Llama3.1-8b-Instruct+SFT+	3.3	0.7	26.0	48.6	25.7	15.3	19.9 _{↑1.3}	31.9	1.5	16.7 _{↓0.1}	68.6 _{↓5.0}	24.6 _{↑0.3}
Llama3.1-8b-Instruct+SPoT	4.0	2.0	27.0	48.6	26.1	16.3	20.7 _{↑2.1}	30.0	7.0	18.5 _{↑1.7}	73.2 _{↓0.4}	26.0 _{↑1.7}

Evaluation We evaluate performance across: *in-domain reasoning*, including AIME24, AIME25, AMC23, Math500 (Hendrycks et al., 2021), Minerva (Lewkowycz et al., 2022), and Olympia (He et al., 2024); *OOD reasoning*, including GPQA-Diamond (GPQA-D) (Rein et al., 2024) and Connect4, and *general instruction following* using IFEval (Zhou et al., 2023). To strictly evaluate OOD reasoning without data contamination, we leverage GAMEBoT (Lin et al., 2025) to dynamically construct the Connect4 dataset (see Appendix E). For reproducibility and fairness, we adopt the evaluation prompts from SoberEval (Hochlehnert et al., 2025). We search for the optimal evaluation hyperparameters for the base models and apply them consistently across all compared methods (see Appendix C).

5.2. Main Results

We compare SPoT against three baselines: (1) **SFT**: supervised fine-tuning on rejection-sampled responses from Gemini 2.5 Pro’s direct answer. (2) **RFT**: rejection sampling fine-tuning using self-generated responses. (3) **SFT+**: supervised fine-tuning on the rectified positive samples y^+ . The main results on Qwen3-8B and Llama-3.1-8B-Instruct are summarized in Table 1. These results reveal the following key observations:

Standard SFT leads to catastrophic forgetting. SFT compromises general capabilities and OOD reasoning. This degradation is even more pronounced on Llama-3.1-8B-Instruct, where IFEval accuracy drops by 11.5 points. Furthermore, the drastic distributional shift between Gemini 2.5 Pro and the policy models erodes even in-domain reasoning (e.g., Qwen3-8B drops from 46.8% to 41.0%). The results confirm that unconstrained likelihood maximization on off-policy data shifts the model too aggressively, damaging its prior knowledge.

Data proximity is necessary but insufficient. Despite

using “surgical” data proximal to the policy model, SFT+ improves in-domain reasoning yet still fails to prevent forgetting in general tasks. Even with more “on-policy” data, RFT yields negligible in-domain improvements but incurs notable forgetting. These results indicate that data proximity alone cannot mitigate the forgetting induced by the standard SFT objective; without explicit regularization (tethering), the model’s broad capabilities inevitably degrade.

SPoT achieves superior reasoning while preserving prior knowledge. SPoT outperforms all baselines across in-domain and OOD metrics, attaining top performance on both Qwen3-8B and Llama-3.1-8B-Instruct. Moreover, SPoT exhibits robust generalization on OOD reasoning and IFEval, even boosting instruction following on Qwen3-8B. This demonstrates the effectiveness of both our surgical data rectification pipeline and the optimization objective.

5.3. Comparison on Loss Objectives

To validate our choice of optimization objective, we conduct experiments using Qwen3-8B to compare SPoT-BCO, SPoT-BCE against DPO, Reward-SFT and DFT (Wu et al., 2025). The results are shown in Table 2.

We observe that both binary classification objectives (SPoT-BCO and SPoT-BCE) outperform other methods. SPoT-BCO yields the best overall average and in-domain reasoning accuracy. The adaptive boundary δ in BCO creates a tighter optimization constraint, pushing the model to clearer decision boundaries on complex math problems. SPoT-BCE serves as a strong alternative, offering superior stability for general capabilities due to strict regularization, achieving the highest scores on IFEval (85.8%) and GPQA-D (49.5%).

In contrast, while DPO successfully mitigates catastrophic forgetting (IFEval 84.7%), it fails to improve in-domain reasoning capabilities. This suggests that preference optimization without fine-grained supervision, is insufficient for

Table 2. **Comparison on loss objectives.** We find that SPoT-BCO yields the best overall results. SPoT-BCE is more competitive on keeping general abilities. DPO mitigates catastrophic forgetting but shows no clear improvements for in-domain reasoning. Although DFT (Wu et al., 2025) is designed for generalization, we observe a clear degradation on OOD tasks.

Model	In-domain Reasoning							OOD Reasoning			General	Avg
	AIME24	AIME25	AMC23	Math500	Minerva	Olympia	Avg	GPQA-D	Connect4	Avg	IFEval	
SPoT-BCO	28.0	27.3	71.5	87.4	39.7	58.5	52.1 ^{↑5.3}	46.8	36.0	41.4 ^{↑11.5}	84.8 ^{↑1.8}	53.3 ^{↑6.2}
SPoT-BCE	33.3	25.3	67.0	87.6	40.1	55.4	51.5 ^{↑4.7}	49.5	31.1	40.3 ^{↑10.4}	85.8 ^{↑2.8}	52.8 ^{↑5.7}
DPO	22.0	19.3	62.5	85.2	40.8	<u>51.6</u>	46.9 ^{↑0.1}	48.9	31.8	40.4 ^{↑10.5}	84.7 ^{↑1.7}	49.6 ^{↑2.5}
Reward-SFT	<u>20.0</u>	<u>16.7</u>	<u>60.5</u>	83.0	<u>39.0</u>	52.3	<u>45.3</u> ^{↓1.5}	49.2	35.2	42.2 ^{↑12.3}	83.7 ^{↑0.7}	48.9 ^{↑1.8}
DFT	24.0	23.3	70.5	<u>82.4</u>	40.4	52.4	48.8 ^{↑2.0}	<u>45.6</u>	<u>3.7</u>	<u>24.7</u> ^{↓5.2}	<u>79.5</u> ^{↓3.5}	<u>46.9</u> ^{↓0.2}

Table 3. **Ablation study on different data.** “Rectified data” refers to the dataset curated using our surgical rectification pipeline, while “direct data” uses the rejected-sampling direct answers from Gemini 2.5 Pro. γ defines the threshold of change ratio in Equation (1).

Model	In-domain Reasoning							OOD Reasoning			General	Avg
	AIME24	AIME25	AMC23	Math500	Minerva	Olympia	Avg	GPQA-D	Connect4	Avg	IFEval	
2k direct data	<u>20.0</u>	<u>14.7</u>	<u>63.0</u>	<u>81.6</u>	<u>37.5</u>	<u>47.6</u>	<u>44.1</u> ^{↓2.7}	<u>42.6</u>	<u>17.2</u>	29.9 ^{↓0.0}	<u>82.6</u> ^{↓0.4}	<u>45.2</u> ^{↓1.9}
2k rectified data, $\gamma = 0.6$	26.0	19.3	67.0	87.8	41.2	52.4	49.0 ^{↑2.2}	49.8	26.0	37.9 ^{↑8.0}	84.1 ^{↑1.1}	50.4 ^{↑3.3}
4k rectified data, $\gamma = 1$	27.3	22.7	64.0	87.6	41.5	58.2	50.2 ^{↑3.4}	49.2	33.3	41.3 ^{↑11.4}	83.6 ^{↑0.6}	51.9 ^{↑4.8}
4k rectified data, $\gamma = 0.6$	28.0	27.3	71.5	87.4	39.7	58.5	52.1 ^{↑5.3}	46.8	36.0	41.4 ^{↑11.5}	84.8 ^{↑1.8}	53.3 ^{↑6.2}

learning correct reasoning paths. Reward-SFT endures forgetting thanks to regularization, yet its in-domain reasoning declines due to the “pull-up” effect. Finally, despite being designed for generalization, DFT exhibits clear degradation against raw SFT objective in our experiments.

5.4. The Effect of the Surgical Rectification Pipeline

We validate the impact of *data proximity* by ablating two key components: the data source and the proximity constraint γ in Section 2. We train Qwen3-8B using the SPoT-BCO objective across all settings, isolating the data curation strategy as the sole variable. The results are summarized in Table 3.

First, training on “rectified data” significantly outperforms “direct data” (+5.2%). Notably, while the SPoT-BCO objective effectively mitigates catastrophic forgetting (only 0.4-point drop on IFEval even with out-of-distribution data), the significant gain in reasoning confirms that proximal data is inherently more effective than out-of-distribution data. Second, scaling the dataset size from 2k to 4k yields consistent improvements. Finally, when controlling for the final training set size, the subset filtered with $\gamma = 0.6$ achieves the highest average score (53.2%), surpassing the unfiltered configuration ($\gamma = 1$). This further confirms that enforcing data proximity is critical for maximizing performance.

6. Related Work

Recent studies indicate that RL mitigates catastrophic forgetting better than SFT by leveraging on-policy data (Shenfeld et al., 2025; Chen et al., 2025). Complementary to this, we highlight the critical role of KL-constrained reward formulation in DPO for preserving knowledge. However, DPO remains sub-optimal for reasoning tasks (Ren & Sutherland,

2025; Azar et al., 2024). Recent works improve DPO via synthetic data refinement (Pal et al., 2024), reference-free objectives (Hong et al., 2024; Meng et al., 2024), iterative DPO (Chen et al., 2024; Pang et al., 2024), and step-level supervision (Lai et al., 2024). In contrast, SPoT resolves these issues by proposing a rectification pipeline to create contrasting pairs and employing a binary loss rather than rank-based objective in DPO. Furthermore, unlike on-policy distillation methods that rely on logit-level supervision (Agarwal et al., 2024; Lu & Lab, 2025), which is unavailable for proprietary LLMs, SPoT utilizes query-based API access without requiring teacher probabilities.

7. Discussion and Conclusion

We demonstrate that it is possible to efficiently boost in-domain performance via supervision without incurring catastrophic forgetting. We present SPoT, a novel paradigm synergizing the *surgical rectification pipeline* with the *binary optimization objective*. Our theoretical and empirical analyses reveal that this loss acts as a sample-wise early stopping mechanism that effectively preserves prior knowledge. We demonstrate that a *binary* objective, as opposed to relative ranking, is critical for rigid reasoning tasks. SPoT also offers the potential to consolidate the complex post-training pipeline (SFT \rightarrow GRPO \rightarrow DPO) into a single phase.

While SPoT reduces reliance on large-scale sampling, it currently requires an Oracle (human or advanced model) for rectification; future work could do experiments with larger models, exploring self-correction mechanisms to remove this dependency. Beyond mathematical reasoning, the principles of surgical rectification and binary verification show promise for domains such as code generation, agentic planning, and reducing hallucinations.

Acknowledgements

This work is supported by Hong Kong Research Grant Council - General Research Fund (Grant No. 17211024) and HKU Seed Fund for PI Research.

Impact Statement

This paper presents work whose goal is to advance the field of Machine Learning. There are many potential societal consequences of our work, none which we feel must be specifically highlighted here.

References

- Achiam, J., Adler, S., Agarwal, S., Ahmad, L., Akkaya, I., Aleman, F. L., Almeida, D., Altenschmidt, J., Altman, S., Anadkat, S., et al. Gpt-4 technical report. *arXiv preprint arXiv:2303.08774*, 2023.
- Agarwal, R., Vieillard, N., Zhou, Y., Stanczyk, P., Garea, S. R., Geist, M., and Bachem, O. On-policy distillation of language models: Learning from self-generated mistakes. In *ICLR*, 2024.
- Anthropic, A. The claude 3 model family: Opus, sonnet, haiku. *Claude-3 Model Card*, 2024.
- Azar, M. G., Guo, Z. D., Piot, B., Munos, R., Rowland, M., Valko, M., and Calandriello, D. A general theoretical paradigm to understand learning from human preferences. In *AISTATS*, 2024.
- Bradley, R. A. and Terry, M. E. Rank analysis of incomplete block designs: I. the method of paired comparisons. *Biometrika*, 39(3/4):324–345, 1952.
- Chen, H., Razin, N., Narasimhan, K., and Chen, D. Retaining by doing: The role of on-policy data in mitigating forgetting. *arXiv preprint arXiv:2510.18874*, 2025.
- Chen, Z., Deng, Y., Yuan, H., Ji, K., and Gu, Q. Self-play fine-tuning converts weak language models to strong language models. In *ICML*, 2024.
- Chu, T., Zhai, Y., Yang, J., Tong, S., Xie, S., Schuurmans, D., Le, Q. V., Levine, S., and Ma, Y. Sft memorizes, rl generalizes: A comparative study of foundation model post-training. In *ICML*, 2025.
- Comanici, G., Bieber, E., Schaekermann, M., Pasupat, I., Sachdeva, N., Dhillon, I., Blistein, M., Ram, O., Zhang, D., Rosen, E., et al. Gemini 2.5: Pushing the frontier with advanced reasoning, multimodality, long context, and next generation agentic capabilities. *arXiv preprint arXiv:2507.06261*, 2025.
- Ethayarajh, K., Xu, W., Muennighoff, N., Jurafsky, D., and Kiela, D. Kto: Model alignment as prospect theoretic optimization. *arXiv preprint arXiv:2402.01306*, 2024.
- He, C., Luo, R., Bai, Y., Hu, S., Thai, Z., Shen, J., Hu, J., Han, X., Huang, Y., Zhang, Y., et al. Olympiadbench: A challenging benchmark for promoting agi with olympiad-level bilingual multimodal scientific problems. In *ACL*, 2024.
- Hendrycks, D., Burns, C., Kadavath, S., Arora, A., Basart, S., Tang, E., Song, D., and Steinhardt, J. Measuring mathematical problem solving with the math dataset. In *NeurIPS Datasets and Benchmarks Track*, 2021.
- Hochlehnert, A., Bhatnagar, H., Udandarao, V., Albanie, S., Prabhu, A., and Bethge, M. A sober look at progress in language model reasoning: Pitfalls and paths to reproducibility. In *COLM*, 2025.
- Hong, J., Lee, N., and Thorne, J. Orpo: Monolithic preference optimization without reference model. In *EMNLP*, 2024.
- Huan, M., Li, Y., Zheng, T., Xu, X., Kim, S., Du, M., Poovendran, R., Neubig, G., and Yue, X. Does math reasoning improve general llm capabilities? understanding transferability of llm reasoning. *arXiv preprint arXiv:2507.00432*, 2025.
- Jung, S., Han, G., Nam, D. W., and On, K.-W. Binary classifier optimization for large language model alignment. In *ACL*, 2025.
- Lai, X., Tian, Z., Chen, Y., Yang, S., Peng, X., and Jia, J. Step-dpo: Step-wise preference optimization for long-chain reasoning of llms. *arXiv preprint arXiv:2406.18629*, 2024.
- Lewkowycz, A., Andreassen, A., Dohan, D., Dyer, E., Michalewski, H., Ramasesh, V., Slone, A., Anil, C., Schlag, I., Gutman-Solo, T., et al. Solving quantitative reasoning problems with language models. In *NeurIPS*, 2022.
- Lin, W., Roberts, J., Yang, Y., Albanie, S., Lu, Z., and Han, K. Gamebot: Transparent assessment of llm reasoning in games. In *ACL*, 2025.
- Lu, K. and Lab, T. M. On-policy distillation. *Thinking Machines Lab: Connectionism*, 2025. doi: 10.64434/tml.20251026. <https://thinkingmachines.ai/blog/on-policy-distillation>.
- Meng, Y., Xia, M., and Chen, D. Simpo: Simple preference optimization with a reference-free reward. In *NeurIPS*, 2024.

- Mukherjee, S., Yuan, L., Hakkani-Tur, D., and Peng, H. Reinforcement learning finetunes small subnetworks in large language models. *arXiv preprint arXiv:2505.11711*, 2025.
- Ouyang, L., Wu, J., Jiang, X., Almeida, D., Wainwright, C., Mishkin, P., Zhang, C., Agarwal, S., Slama, K., Ray, A., et al. Training language models to follow instructions with human feedback. In *NeurIPS*, 2022.
- Pal, A., Karkhanis, D., Dooley, S., Roberts, M., Naidu, S., and White, C. Smaug: Fixing failure modes of preference optimisation with dpo-positive. *arXiv preprint arXiv:2402.13228*, 2024.
- Pang, R. Y., Yuan, W., He, H., Cho, K., Sukhbaatar, S., and Weston, J. Iterative reasoning preference optimization. In *NeurIPS*, 2024.
- Rafailov, R., Sharma, A., Mitchell, E., Manning, C. D., Ermon, S., and Finn, C. Direct preference optimization: Your language model is secretly a reward model. In *NeurIPS*, 2023.
- Rafailov, R., Hejna, J., Park, R., and Finn, C. From r to q*: Your language model is secretly a q-function. In *COLM*, 2024.
- Rein, D., Hou, B. L., Stickland, A. C., Petty, J., Pang, R. Y., Dirani, J., Michael, J., and Bowman, S. R. Gpqa: A graduate-level google-proof q&a benchmark. In *COLM*, 2024.
- Ren, Y. and Sutherland, D. J. Learning dynamics of llm finetuning. In *ICLR*, 2025.
- Shao, Z., Wang, P., Zhu, Q., Xu, R., Song, J., Bi, X., Zhang, H., Zhang, M., Li, Y., Wu, Y., et al. Deepseekmath: Pushing the limits of mathematical reasoning in open language models. *arXiv preprint arXiv:2402.03300*, 2024.
- Shenfeld, I., Pari, J., and Agrawal, P. RL’s razor: Why online reinforcement learning forgets less. *arXiv preprint arXiv:2509.04259*, 2025.
- Wagner, R. A. and Fischer, M. J. The string-to-string correction problem. *Journal of the ACM (JACM)*, 21(1): 168–173, 1974.
- Wang, W., Chen, Z., Wang, W., Cao, Y., Liu, Y., Gao, Z., Zhu, J., Zhu, X., Lu, L., Qiao, Y., et al. Enhancing the reasoning ability of multimodal large language models via mixed preference optimization. *arXiv preprint arXiv:2411.10442*, 2024.
- Wu, Y., Zhou, Y., Ziheng, Z., Peng, Y., Ye, X., Hu, X., Zhu, W., Qi, L., Yang, M.-H., and Yang, X. On the generalization of sft: A reinforcement learning perspective with reward rectification. *arXiv preprint arXiv:2508.05629*, 2025.
- Yang, A., Li, A., Yang, B., Zhang, B., Hui, B., Zheng, B., Yu, B., Gao, C., Huang, C., Lv, C., et al. Qwen3 technical report. *arXiv preprint arXiv:2505.09388*, 2025.
- Yu, Q., Zhang, Z., Zhu, R., Yuan, Y., Zuo, X., Yue, Y., Dai, W., Fan, T., Liu, G., Liu, L., et al. Dapo: An open-source llm reinforcement learning system at scale. *arXiv preprint arXiv:2503.14476*, 2025.
- Yue, Y., Chen, Z., Lu, R., Zhao, A., Wang, Z., Song, S., and Huang, G. Does reinforcement learning really incentivize reasoning capacity in llms beyond the base model? *arXiv preprint arXiv:2504.13837*, 2025.
- Zhou, J., Lu, T., Mishra, S., Brahma, S., Basu, S., Luan, Y., Zhou, D., and Hou, L. Instruction-following evaluation for large language models. *arXiv preprint arXiv:2311.07911*, 2023.

A. Extended Related Work

Catastrophic Forgetting Recent work highlights a divergence between SFT and RL: while SFT is prone to overfitting and catastrophic forgetting, RL demonstrates superior generalization (Chu et al., 2025; Huan et al., 2025). To explain this, Mukherjee et al. (2025) observed that RL updates are typically sparse, affecting only specific parameter subnetworks, whereas SFT triggers dense, global updates. Alternatively, Shenfeld et al. (2025) and Chen et al. (2025) argued that on-policy data generation—rather than the optimization objective—is the primary driver of knowledge retention. However, our analysis in Section 3 suggests that the optimization objective remains critical; specifically, the implicit regularization (KL-constraint) inherent in reward-based objectives is essential for preserving prior knowledge.

DPO for Reasoning DPO tends to overly penalize rejected responses rather than strengthening the chosen ones (Ren & Sutherland, 2025; Azar et al., 2024; Pal et al., 2024), making it sub-optimal for reasoning. To mitigate this, several variants have emerged: Azar et al. (2024) introduced IPO to regularize against overfitting; Pal et al. (2024) and Meng et al. (2024) encouraged a larger margin to incentivize learning from positive examples; and others (Hong et al., 2024; Wang et al., 2024) integrated SFT objectives to reinforce preferred responses.

Furthermore, methods such as KTO (Ethayarajh et al., 2024) and BCO (Jung et al., 2025) utilize unpaired or binary feedback to reduce annotation costs. While BCO was originally designed for data efficiency, we demonstrate through theoretical and empirical analysis that its loss structure is uniquely suited to address the ranking inefficiencies of DPO while mitigating catastrophic forgetting during post-training for reasoning.

Beyond general alignment, other works also leverage DPO to enhance reasoning capabilities. Chen et al. (2024) and Pang et al. (2024) employed iterative self-improvement, distinguishing model generations from human data. Lai et al. (2024) introduced Step-DPO including a data rectification pipeline for precise step-level feedback. SPOT distinguishes itself from Step-DPO in two critical aspects. First, while Step-DPO relies on self-correction—which is limited by the model’s intrinsic capabilities—we employ an Oracle-guided correction pipeline. Second, whereas Step-DPO retains the standard DPO objective, SPOT utilizes a reward-based binary cross-entropy objective. This approach more effectively addresses the sub-optimality of DPO for reasoning while mitigating forgetting in the post-training phase.

Online Policy Distillation SPOT can be viewed as a form of online policy distillation, as it learns to recover from self-generated errors under teacher supervision. Agarwal et al. (2024); Lu & Lab (2025) demonstrated that applying teacher supervision to student-generated trajectories enables rapid alignment and error correction, avoiding the inefficiency associated with full RL. However, these methods typically rely on logit-level supervision from the teacher model, which is often unavailable due to the proprietary nature of state-of-the-art LLMs. In contrast, SPOT operates on query-based API access without requiring teacher probabilities. Furthermore, SPOT utilizes a distinct regularized optimization objective for mitigating catastrophic forgetting.

B. Breaking the Oracle’s Capability Ceiling

A natural concern regarding SPOT lies in its dependency on the Oracle model. Intuitively, in standard distillation paradigms, the policy model’s performance is hypothesized to be upper-bounded by the capabilities of the Oracle (teacher). However, when provided with the ground truth, SPOT mitigates this by redefining the Oracle’s role from open-ended problem solving to **reference-guided error correction**. By providing the Oracle with both the policy-generated error and the ground truth, the computational burden shifts from rectifying a reasoning chain from scratch to bridging the gap between the error and the correct answer. Consequently, the policy model can learn from corrected trajectories that the Oracle itself might not have been capable of generating, effectively allowing the student to surpass the teacher’s generative ceiling. This also allows self-improving when setting the Oracle to be the policy model itself.

C. Hyperparameter Setting

For data generation and evaluation, we employ a temperature of 0.7 and top- p of 0.8, with a maximum token limit of 32,768. We train all models for 2 epochs with a context length of 8,192 and $\beta = 0.1$. To ensure a fair comparison, we systematically tune the hyperparameters for the baselines. Regarding learning rates, SPOT utilizes 1×10^{-6} for Qwen3-8B and 2×10^{-7} for Llama3.1-8B-Instruct. For SFT, RFT, and SFT+, we use learning rates of 5×10^{-6} (Qwen3-8B) and 1×10^{-6} (Llama3.1-8B-Instruct). The batch size is set to 32 for all the methods.

D. Change Ratio of Rectification

We visualize the distributions of change ratio, which measures the proportion of the reasoning chain that was modified during rectification. We calculate this ratio based on the edit distance between the original and rectified responses. The results are shown in Figure 5.

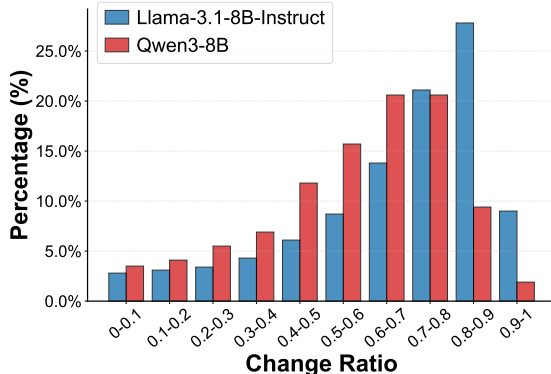


Figure 5. **Distributions of change ratio.** A higher change ratio indicates that reasoning failures occur earlier in the reasoning chain. The distribution shape is determined by the model ability and the data difficulty together.

E. Connect4 Task

Game Rules Connect4 is a two-player game of perfect information played on a vertical grid of dimension 6×7 . Players alternate turns dropping distinct pieces into one of the seven columns, where the piece occupies the lowest available row within that column due to simulated gravity. The objective is to form a contiguous line of four pieces either vertically, horizontally, or diagonally. It requires the LLM to *parse the board state*, *execute lookahead planning*, and *identify winning topologies*. With a state-space complexity of approximately 4.5×10^{12} legal positions, Connect4 offers a non-trivial, deterministic environment ideal for generating synthetic states to evaluate LLMs without data contamination.

Dynamic Dataset Construction To strictly evaluate OOD reasoning without the risk of data contamination in static benchmarks, we leverage the GAMEBoT framework (Lin et al., 2025). While GAMEBoT supports full-game simulations, interactive evaluation is often inefficient and difficult to reproduce. Instead, we dynamically construct a static dataset of reasoning tasks rooted in Connect4. To ensure the model relies on symbolic reasoning, the board state is serialized into a text-based format (e.g., a list of coordinates).

The construction process involves:

- **State Generation:** We utilize two randomized agents to simulate gameplay, generating a diverse distribution of board states ranging from balanced positions to critical tactical scenarios.
- **Filtering and Balancing:** We filter out duplicate states. Furthermore, to prevent LLMs from inflating scores by consistently predicting “no winning moves” (due to label imbalance), we downsample states with empty answers, maintaining them at a maximum ratio of 20% of the dataset.
- **Dataset Compilation:** For efficient evaluation, we construct a final dataset comprising 500 distinct instances.

Evaluation Protocol For each instance, LLMs are prompted to solve two problems in a query:

- *Are there any potential winning moves to form 4-in-a-row for you? Output all winning moves.*
- *Are there any potential winning moves to form 4-in-a-row for your opponent? Output all winning moves.*

Ground truth is computed using a perfect solver within GAMEBoT. We parse the model’s Chain-of-Thought (CoT) to extract the final answers and verify them against the game engine’s ground truth.

F. Rectification Prompt

Rectification Prompt Without Ground Truth

Act as a helpful teaching assistant. Your goal is to revise a student model's answer to make it correct, while maintaining the student model's original writing style, tone, and formatting. The final result should look as if the student model had solved the problem correctly on its first try.

You should first solve the problem independently and do the following:

1. Identify the correct parts of the student model's answer and keep them.
2. Replace the incorrect parts with correct reasoning.
3. Carefully match the student model's original writing style, including their tone, vocabulary, formatting and sentence structure.

****IMPORTANT OUTPUT FORMAT:****

1. First output ``=== CORRECTED STARTED ==='' followed by the corrected answer
2. Ends with the corrected answer in the format: 'Therefore, the final answer is: $\boxed{\text{ANSWER}}$.'
3. Then output ``=== CORRECTED ENDED ==='' at the end of the corrected trace
4. Do not output meta-phrases like "Here is the corrected version"

Rectification Prompt With Ground Truth

Act as a helpful teaching assistant. Your goal is to revise a student model's answer to make it correct, while maintaining the student model's original writing style, tone, and formatting. The final result should look as if the student model had solved the problem correctly on its first try.

You should compare the student model's answer with the Reference Ground Truth and do the following:

1. Identify the correct parts of the student model's answer and keep them.
2. Replace the incorrect parts with correct reasoning.
3. Carefully match the student model's original writing style, including their tone, vocabulary, and sentence structure.

****IMPORTANT OUTPUT FORMAT:****

1. First output ``=== CORRECTED STARTED ==='' followed by the corrected answer
2. Ends with the corrected answer in the format: 'Therefore, the final answer is: $\boxed{\text{ANSWER}}$.'
3. Then output ``=== CORRECTED ENDED ==='' at the end of the corrected trace
4. Do not output meta-phrases like "Here is the corrected version"

G. Rectification Samples

1 To solve the problem of how many different rectangles with sides parallel to the grid can be formed by connecting four of the dots in a 4×4 square array of dots, we can approach it step by step. Step 1: Understand the Grid. We are given a 4×4 square array of dots, which means there are 4 rows and 4 columns of dots. The dots are arranged in a grid with horizontal and vertical spacing. A rectangle is formed by choosing two distinct horizontal lines and two distinct vertical lines that form the sides of the rectangle. So, the problem reduces to: How many ways can we choose 2 horizontal lines and 2 vertical lines from the grid? Step 2: Count the Number of Horizontal and Vertical Lines. In a 4×4 grid of dots, there are 5 horizontal lines (since 4 dots mean 3 spaces between them, and we count the top and bottom lines as well). Similarly, there are 5 vertical lines. So, we are choosing 2 lines from 5 in both directions. Step 3: Use Combinations. The number of ways to choose 2 lines from 5 is given by the combination formula: $\binom{5}{2} = \frac{5!}{2! \cdot 3!} = 10$. So, we can choose 10 pairs of horizontal lines and 10 pairs of vertical lines. Each pair of horizontal and vertical lines defines a unique rectangle. Step 4: Multiply the Combinations. To find the total number of rectangles: $\binom{5}{2} \times \binom{5}{2} = 10 \times 10 = 100$. Final Answer: $\boxed{100}$. Therefore, the final answer is: $\boxed{100}$.

1 To solve the problem of how many different rectangles with sides parallel to the grid can be formed by connecting four of the dots in a 4×4 square array of dots, we can approach it step by step. Step 1: Understand the Grid. We are given a 4×4 square array of dots, which means there are 4 rows and 4 columns of dots. The dots are arranged in a grid with horizontal and vertical spacing. A rectangle is formed by choosing two distinct horizontal lines and two distinct vertical lines that form the sides of the rectangle. So, the problem reduces to: How many ways can we choose 2 horizontal lines and 2 vertical lines from the grid? Step 2: Count the Number of Horizontal and Vertical Lines. In a 4×4 grid of dots, there are 4 horizontal lines that can be drawn through the rows of dots. Similarly, there are 4 vertical lines that can be drawn through the columns of dots. So, we are choosing 2 lines from 4 in both directions. Step 3: Use Combinations. The number of ways to choose 2 lines from 4 is given by the combination formula: $\binom{4}{2} = \frac{4!}{2! \cdot 2!} = 6$. So, we can choose 6 pairs of horizontal lines and 6 pairs of vertical lines. Each pair of horizontal and vertical lines defines a unique rectangle. Step 4: Multiply the Combinations. To find the total number of rectangles: $\binom{4}{2} \times \binom{4}{2} = 6 \times 6 = 36$. Final Answer: $\boxed{36}$. Therefore, the final answer is: $\boxed{36}$.

Figure 6. Random Rectification Example 1. Left: answer from Qwen3-8B; Right: rectification by Gemini 2.5 Pro.

1 We are given two geometric sequences: First sequence: $16, a_1, a_2, \dots$ Second sequence: $56, b_1, b_2, \dots$ Both sequences have the same common nonzero ratio, say r . We are also given: $a_{2023} = b_{2020}$. We are to compute: $b_6 - a_6$. Step 1: Express terms of the sequences. Let $a_n = 16 \cdot r^{n-1}$. First term: 16 . Common ratio: r . General term: $a_n = 16 \cdot r^{n-1}$. So: $a_{2023} = 16 \cdot r^{2022}$. Second sequence: First term: 56 . Common ratio: r . General term: $b_n = 56 \cdot r^{n-1}$. So: $b_{2020} = 56 \cdot r^{2019}$. Step 2: Use the given condition. We are told: $a_{2023} = b_{2020}$. Substitute the expressions: $16 \cdot r^{2022} = 56 \cdot r^{2019}$. Divide both sides by r^{1999} (since $r \neq 0$): $16 \cdot r^3 = 56$. Now solve for r^3 : $r^3 = \frac{56}{16} = \frac{7}{2}$. Step 3: Compute $b_6 - a_6$. We now compute the 6th terms of both sequences: $a_6 = 16 \cdot r^5$, $b_6 = 56 \cdot r^5$. So: $b_6 - a_6 = (56 - 16) \cdot r^5 = 40 \cdot r^5$. We already know that: $r^3 = \frac{7}{2}$. $r^5 = r^3 \cdot r^2 = \frac{7}{2} \cdot r^2$. We need to find r^2 . Let's express r^5 in terms of r^3 : $r^5 = r^3 \cdot r^2 = \frac{7}{2} \cdot r^2$. $\frac{7}{2} \cdot r^2 = 40 \cdot \frac{7}{2} \cdot r^2$. Instead, we can use the fact that: $r^3 = \frac{7}{2}$. $r = \left(\frac{7}{2}\right)^{1/3}$. So: $r^5 = \left(\frac{7}{2}\right)^{5/3}$. Then: $b_6 - a_6 = 40 \cdot \left(\frac{7}{2}\right)^{5/3}$. Step 4: Final expression. We are to compute: $b_6 - a_6 = 40 \cdot \left(\frac{7}{2}\right)^{5/3}$. This is the final expression. If a numerical value is required, we can compute it numerically, but the question asks to compute $b_6 - a_6$, and we have done so in terms of r , so the final answer is: $\boxed{40 \cdot \left(\frac{7}{2}\right)^{5/3}}$. Therefore, the final answer is: $\boxed{40 \cdot \left(\frac{7}{2}\right)^{5/3}}$.

1 We are given two geometric sequences: First sequence: $16, a_1, a_2, \dots$ Second sequence: $56, b_1, b_2, \dots$ Both sequences have the same common nonzero ratio, say r . We are also given: $a_{2023} = b_{2020}$. We are to compute: $b_6 - a_6$. Step 1: Express terms of the sequences. Let $a_n = 16 \cdot r^{n-1}$. First term: 16 . Common ratio: r . General term: $a_n = 16 \cdot r^{n-1}$. So: $a_{2023} = 16 \cdot r^{2022}$. Second sequence: First term: 56 . Common ratio: r . General term: $b_n = 56 \cdot r^{n-1}$. So: $b_{2020} = 56 \cdot r^{2019}$. Step 2: Use the given condition. We are told: $a_{2023} = b_{2020}$. Substitute the expressions: $16 \cdot r^{2022} = 56 \cdot r^{2019}$. Divide both sides by r^{1999} (since $r \neq 0$): $16 \cdot r^3 = 56$. Now solve for r^3 : $r^3 = \frac{56}{16} = \frac{7}{2}$. Step 3: Compute $b_6 - a_6$. We now compute the terms a_6 and b_6 using our general formulas from Step 1. $a_6 = 16 \cdot r^5$, $b_6 = 56 \cdot r^5$. So the difference is: $b_6 - a_6 = 56 \cdot r^5 - 16 \cdot r^5 = (56 - 16) \cdot r^5 = 40 \cdot r^5$. We need to find the value of r^5 . We already know from Step 2 that: $r^3 = \frac{7}{2}$. We can get r^6 by squaring r^3 : $r^6 = \left(\frac{7}{2}\right)^2 = \frac{49}{4}$. We can substitute this value back into our expression for the difference: $b_6 - a_6 = 40 \cdot r^6 = 40 \cdot \frac{49}{4} = 490$. Let's simplify this: $b_6 - a_6 = \frac{40}{4} \cdot 49 = 10 \cdot 49 = 490$. Therefore, the final answer is: $\boxed{490}$.

Figure 9. Random Rectification Example 4. Left: answer from Qwen3-8B; Right: rectification by Gemini 2.5 Pro.